Forestry An International Journal of Forest Research

Institute of Chartered Foresters

Forestry 2015; **88**, 622–632, doi:10.1093/forestry/cpv030
Advance Access publication 25 August 2015

Annual ring density for lodgepole pine as derived from models for earlywood density, latewood density and latewood proportion

Derek F. Sattler[1], Chris Finlay[1] and James D. Stewart[2]*

[1]*Foothills Research Institute, Hinton, Alberta, Canada*
[2]*Canadian Wood Fibre Centre, Canadian Forest Service, Natural Resources Canada, Edmonton, Alberta, Canada*

*Corresponding author. Tel: +01 7804357224; Fax: +01 7804357359; E-mail: jim.d.stewart@canada.ca

Received 18 December 2014

Model-based prediction of annual ring density (RD) is necessary to manage forests for wood quality objectives. However, annual RD in lodgepole pine (*Pinus contorta* Dougl. ex Loud.) exhibits a high degree of variability making it a challenge to model. We compared two methods of predicting annual RD including (1) a ring component approach and (2) a direct approach. The former approach uses model-based estimates of earlywood density (EWD), latewood density (LWD) and latewood proportion (LWP) to calculate annual RD. The latter approach uses a single model with annual RD as the dependent variable. The two approaches were tested using a dataset which included sites on the western and eastern slopes of the Rocky Mountains, within the provinces of British Columbia and Alberta, Canada. The best models for EWD, LWD and LWP included ring number and ring width, while site-specific parameters indicated that sites on the western slopes differed from those on the eastern slopes. Component-based estimates of annual RD using only fixed effects explained 25 per cent of the variability, increasing to 63 per cent with random effects. The best model for a direct estimate of annual RD explained only 5 per cent of the variability using fixed effects, increasing to 55 per cent with random effects.

Introduction

Among the various wood properties affecting the yield and quality of end-use products, wood density is largely acknowledged as being the most important for several pine species, including red pine (*Pinus resinosa* Ait.) (Larocque and Marshall, 1995), jack pine (*P. banksiana* Lamb.) (Barbour *et al.*, 1994) and Scots pine (*P. sylvestris* L.) (Wilhelmsson *et al.*, 2002). As noted by Middleton *et al.* (1995), this is also true for lodgepole pine (*P. contorta* Dougl. ex Loud.), a species of high commercial importance within Alberta and British Columbia, Canada. Given the importance of wood density, the variation in annual mean ring density (RD) from pith to bark is of substantial interest to forest managers and the forestry wood supply chain.

At the anatomical level, density is a function of cell size, shape and the thickness of the cell walls (Wang and Aitken, 2001). At the ring-level, wood density may be determined through a combination of earlywood density (EWD), latewood density (LWD), ring width (RW) and the relative proportions of EWD and LWD (EWP and LWP, respectively). Estimates of annual RD may, therefore, be obtained by developing separate models for EWD, LWD and either latewood or earlywood proportion. This method may be referred to as the component model approach. However, the most common approach to obtain predictions of annual RD has been to simply develop a model where annual RD is the dependent variable, i.e. a single model provides a direct estimate of annual RD. Examples include the recent models by Schneider *et al.* (2008) for jack pine and Auty *et al.* (2014) for Scots pine. Because of its simplicity, the direct approach facilitates the process of integration into tree growth simulators which operate on an annual time scale.

However, the decision of whether to develop a model which provides a direct estimate of annual RD or to use a component model approach is strongly influenced by two factors. If individual trees tend to display a similar pith-to-bark pattern for annual RD, then a direct estimate of annual RD may be possible. This is because the similarity in the pith-to-bark pattern facilitates the construction of a simple model that is generalizable to the population. However, if the pith-to-bark pattern for annual RD is complex, then the number of parameters used to describe the pattern may increase to a point that the model is overfitted, thus limiting the application of the model to new datasets.

For lodgepole pine, the typical pith-to-bark pattern for annual RD is complex. It includes a sharp decline from the pith, a gradual increase through the juvenile – mature wood transition zone, and finally an asymptotic tendency within the mature wood section of the stem (Mansfield *et al.*, 2007;2009). Furthermore, Peng and Stewart (2013) note that this pattern seems to hold only generally across the landscape. The same study also reported that lodgepole pine displayed high inter-annual variability in RD.

To address these modelling issues, Peng and Stewart (2013) used the 5-year average RD to develop a model for the direct prediction of annual RD in lodgepole pine. Fitting the model to the 5-year average RD had the effect of smoothing out the inter-annual variability, thereby facilitating parameter estimation.

However, to accommodate the divergence in the pith-to-bark patterns among sites, a complex equation form was required which included distance from pith, three covariates for RW and random effects at the site and tree-level. A validation of the model suggested that if the random effects at the site level can be calibrated for a new dataset, then predictions of annual RD are expected to be reasonably close to actual values. However, if calibration is not possible, then the model is expected to perform poorly.

A component model approach to estimate annual RD in lodgepole pine has yet to be presented. Using such an approach presents potential advantages over the direct estimation of annual RD. For example, if the individual components of annual RD show greater similarity in their pith-to-bark patterns than annual RD itself, it may be easier to find equation forms that can be generalized to the geographic area of interest. A component modelling approach can also accommodate the variable response of wood density to changes in RW within the same growing season. Wang *et al.* (2000), for example, reported that the pith-to-bark development of annual RD in lodgepole pine is negatively correlated with RW. However, at the intra-annual ring level, Wang and Aitken (2001) reported that ring area showed a significant negative correlation with EWD but was unrelated to changes in LWD. Evidence from other pine species also suggests that the magnitude and direction (i.e. positive or negative) of the effect of RW varies among the individual components of annual RD. Larocque and Marshall (1995), for example, noted that RW had a stronger negative relationship with annual EWD than with annual LWD in red pine. When examining Scots pine, Peltola *et al.* (2007) found that while increased growth rate led to increases in both earlywood width (EWW) and latewood width (LWW), there was a decrease in annual EWD and an increase in annual LWD. Finally, Schneider *et al.* (2008) reported that changes in RW had a significant effect on annual RD in jack pine. However, for both EWD and LWD, the effect of RW was weak, with changes in annual latewood proportion (LWP) cited as the main pathway through which RW affected annual RD. Based on this evidence, testing the use of a component model approach for the prediction of annual RD in lodgepole pine seems to be warranted.

The objectives of the current study were to: (1) develop models for annual EWD, LWD, LWP and RD, and (2) contrast estimates of annual RD from a component model approach to those from a direct approach. The data used to develop these models comes from sites located on the western and eastern slopes of the Canadian Rocky Mountains. While lodgepole pine is commonly found on both the western and eastern slopes, regional differences in climate exist and may partially explain differences in the pith-to-bark patterns for EWD, LWD LWP and RD. Therefore, an additional objective of this study was to investigate the presence of regional differences for each of the models. Ultimately, the models derived from this study will be programmed into software that uses the output from individual tree-growth simulators. These models will, therefore, be available for forest managers to use when assessing the effects of growing conditions under various stand management scenarios.

Methods

Measurements and model dataset

Data used for this study were obtained from six long-term silvicultural research trials. Four of the sites are located east of the North American continental divide, in the central foothills of Alberta (Teepee North (TN), Teepee Flat (TF), MacKay (MK) and McCardell (MC)). The remaining two sites are located in south-eastern British Columbia (Cranbrook (CR) and Parsons (PA)), west of the continental divide. The sites are spread over a wide geographic area, with the maximum distance between two sites being ~650 km (MK to CR). Only two sites are separated by <200 km, with the TN and TF sites lying <5 km apart. At the site level, the soil nutrient and moisture regimes are similar. In terms of nutrients, all sites are either medium, medium-rich or medium poor. Likewise, local soil moisture regime is either submesic or mesic. At a regional level, there are well recognized differences in climate between the eastern and western slopes. Most notably, the eastern slopes of the Rocky Mountains are drier and cooler than those west of the continental divide, which is a result of the rain shadow effect of the mountains. For a more detailed description of site conditions, readers should consult Whitehead and Russo (2005) and Stewart *et al.* (2006).

Thinning treatments had been applied at each of the sites, with the McCardell site having undergone both thinning and fertilizer treatments. The number of trees sampled, the age and diameter at breast height (DBH) of the trees, and summary statistics for wood density and annual RW are presented in Table 1. Although the trees varied in total age, all were at least 40 years cambial age at breast height (BH). From each thinning treatment (or combination of thinning and fertilizer treatment), 15 trees were randomly selected for sampling (see Peng and Stewart 2013 for a more detailed description of the data collection methods). Samples consisted of either a core or a disc taken at BH. Following preparation, the wood samples were scanned from pith to bark using a SilviScan-3 instrument (Evans, 1994; Defo *et al.*, 2009), from which measures of annual RD, EWD, LWD, EWW and LWW were obtained. Scanning resolution was set at 0.025 mm. For demarcation of the earlywood–latewood boundary, we used the mean of the maximum and minimum density within a given annual ring. The model-fitting dataset was created by pooling measurements from all six sites.

Statistical analysis

To estimate annual RD using a component model approach, separate models were developed for annual EWD, LWD and LWP. Our selection of component models to be developed was based on the following relationship with annual RD:

$$\mathrm{RD}_k = \frac{(\mathrm{EWD}_k \times \mathrm{EWW}_k) + (\mathrm{LWD}_k \times \mathrm{LWW}_k)}{(\mathrm{RW}_k)}, \tag{1}$$

where k is the kth annual ring from pith and all other symbols are as previously defined. Simplifying equation (1) we obtain

$$\mathrm{RD}_k = \mathrm{EWD}_k \times \mathrm{EWP}_k + \mathrm{LWD}_k \times \mathrm{LWP}_k, \tag{2}$$

where EWP and LWP are earlywood proportion and latewood proportion for the kth annual ring, respectively. Equation (2) can further be simplified to

$$\mathrm{RD}_k = \mathrm{EWD}_k \times (1 - \mathrm{LWP}_k) + \mathrm{LWD}_k \times \mathrm{LWP}_k. \tag{3}$$

Although silvicultural treatments had been applied to the sites, we did not explicitly consider these treatments in our modelling approach. Previous studies on Scots pine (Peltola *et al.*, 2007; Mäkinen and Hynynen, 2014) found thinning and fertilizer treatments to have little to no effect on mean intra- or annual RD. Therefore, for the current study we assumed that there was no direct effect of thinning on the individual components of annual RD. Similar to Peltola *et al.* (2007) and Mäkinen and Hynynen (2014), preliminary analyses of our data indicated a significant treatment effect on post-thinning annual RW at all six sites. Specifically, annual RW

Table 1 Site and tree information for the model-fitting dataset with standard deviation in parentheses ( ) and minimum and maximum in braces { }

Site and location	No. of trees	No. of rings	Mean age (at 1.3 m)	DBH (cm)	MRW (mm year^{-1})	Nutrient/moisture regime
CR 49°25.0′N, 115°37.1′W	57	3594	82 (2.67) {80–85}	20.28 (3.71) {17.65–22.91}	1.13 (0.12) {1.04–1.21}	Medium-poor/mesic–submesic
PA 50°59.3′N, 116°41.2′W	30	1807	85 (1.03) {84–86}	22.43 (1.82) {21.14–23.72}	1.22 (0.16) {1.11–1.34}	Medium/mesic
MK 53°32.7′N, 115°32.3′W	41	2368	62 (1.3) {61–64}	12.50 (2.10) {10.58–14.74}	1.21 (0.24) {0.96–1.45}	Medium-poor/mesic
TF 51°54.1′N, 115°11.2′W	43	2098	55 (0.60) {54–56}	12.42 (1.52) {11.09–13.97}	1.24 (0.21) {1.12–1.49}	Medium-rich/mesic
MC 53°11.8′N, 117°11.1′W	79	3732	52 (0.16) {52–53}	14.23 (0.24) {14.44–14.80}	1.34 (0.03) {1.32–1.36}	Medium-poor/mesic
TN 51°53.8′N, 115°09.7′W	44	2282	54 (1.85) {53–57}	12.31 (1.47) {10.64–13.60}	1.41 (0.23) {1.19–1.65}	Medium/submesic

DBH = diameter at breast height, MRW = mean ring width. The Cranbrook (CR) and Parsons (PA) sites are on the western slopes of the Rockies, while MacKay (MK), Teepee Flat (TF), McCardell (MC) and Teepee North (TN) are on the eastern slopes.

increased with increasing thinning intensity. Therefore, if there was an effect of silvicultural treatment on RD or its components, this effect could be captured indirectly through RW. As a final measure of assurance that thinning treatments were not directly affecting the components of annual RD, residuals from the final models were inspected for bias across thinning treatments.

Given the different pith-to-bark patterns at the site-level for EWD, LWD and LWP, various equation forms were screened. The screening process involved fitting the potential equations to the model dataset and evaluating model performance using the Akaike information criterion (AIC) (Akaike, 1974). All equations that were considered during the initial screening process contained RN as the sole covariate. The screening process provided a set of starting-point equations on which further model testing was performed. The starting point equations for EWD, LWD and LWP were

$$\mathrm{EWD}_{ijk} = \beta_0 \times \exp[-(\beta_1 + b_{1,i} + b_{1,ij}) \times \mathrm{RN}_{ijk}] + \frac{(\beta_2 + b_{2,i} + b_{2,ij}) \times \mathrm{RN}_{ijk}}{[(\beta_3 + b_{3,i} + b_{3,ij}) + \mathrm{RN}_{ijk}]} + \varepsilon_{ijk}, \tag{4}$$

$$\mathrm{LWD}_{ijk} = \gamma_0 \times \exp(-\gamma_1 \times \mathrm{RN}_{ijk}) + (\gamma_2 + c_{2,i} + c_{2,ij}) \times \mathrm{RN}_{ijk} + (\gamma_3 + c_{3,i} + c_{3,ij}) + \varepsilon_{ijk}, \tag{5}$$

$$\mathrm{LWP}_{ijk} = (\delta_0 + d_{0,i} + d_{0,ij}) + \frac{\delta_1 + d_{1,i} + d_{1,ij}}{1 + \exp\left[\frac{(\delta_2 + d_{2,i} + d_{2,ij} - RN_{ijk})}{\delta_3 + d_{3,i} + d_{3,ij}}\right]} + \varepsilon_{ijk} \tag{6}$$

where β_0 to β_3, γ_0 to γ_3 and δ_0 to δ_3 are the fixed-effect parameters for the respective models and RN_{ijk} is the ring number (RN) at BH for the kth annual ring from pith, from the jth tree within the ith site. The variance components of the random effects are represented by $b_{1,i}$, $b_{1,ij}$, $b_{2,i}$, $b_{2,ij}$, $b_{3,i}$ and $b_{3,ij}$ for equation (4) (EWD), $c_{2,i}$, $c_{2,ij}$, $c_{3,i}$ and $c_{3,ij}$ for equation (5) (LWD), and $d_{0,i}$, $d_{0,ij}$, $d_{1,i}$, $d_{1,ij}$, $d_{3,i}$ and $d_{3,ij}$ for equation (6) (LWP). The error term for each equation, ε_{ijk}, is assumed to follow a normal distribution. When fitting the models, we used a continuous autoregressive correlation structure to account for correlation between annual rings within a tree.

As a point of comparison for the component model approach, an equation for the direct estimate of annual RD was also developed. Using the same model screening criteria, the starting-point equation selected for the direct estimate of annual RD was

$$\mathrm{RD}_{ijk} = \phi_0 \times \exp[-(\phi_1 + g_{1,i} + g_{1,ij}) \times \mathrm{RN}_{ijk}] + \frac{(\phi_2 + g_{2,i} + g_{2,ij}) \times \mathrm{RN}_{ijk}}{[(\phi_3 + g_{3,i} + g_{3,ij}) + \mathrm{RN}_{ijk}]} + \varepsilon_{ijk}, \tag{7}$$

where ϕ_0 to ϕ_3 are the fixed-effect parameters, $g_{1,i}$, $g_{1,ij}$, $g_{2,i}$, $g_{2,ij}$, $g_{3,i}$ and $g_{3,ij}$ are the variance components of the random effects and all other variables are as previously defined. The random effects for all equations were assumed to be normally distributed. Using equation (4) as an example, this implies that the random effects are distributed as $b_i \sim N(0,\Psi_1)$ and $b_{ij} \sim N(0,\Psi_2)$, where Ψ_1 and Ψ_2 are the variance–covariance matrices associated with the site and tree-level random effects and where tree-level random effects are assumed to be independent of site-level random effects.

For equations (4) and (7), the leading exponential function describes the initial decrease in EWD and RD, respectively, from the pith. To this, we added the Michaelis–Menten function which describes the gradual increase towards a maximum value which is controlled by the β_2 and ϕ_2 parameters in the respective equations. Equation (5) is composed of an exponential function which describes the initial increase from the pith to which a linear equation that has been added to represent the long-term decay in

LWD as RN increases. Finally, equation (6) is a logistic function which describes the tendency for LWP to show a sigmoidal trend from pith to bark, where the parameter δ_1 represents the asymptote as RN gets large. As it is currently formulated, predictions from equation (6) are not bounded to lie between 0 and 1. One may impose bounds through transformation of the dependent variable or by fitting the model using a logit link function and a binomial distribution. However, the distribution of LWP in the model dataset data fell well within the 0–1 range. Therefore, no bounds were used and model predictions are expected to lie between 0 and 1.

Ring width and site effects

Our next step was to test whether the variation in annual EWD, LWD, LWP and RD which was not explained by RN could be explained through changes in radial growth rate. A covariate for RW was, therefore, systematically tested as an additive effect on each fixed-effect parameter in equations (4)–(7). The best model for each component was selected with the aid of AIC and a likelihood ratio test between the fitted model and the next best model. Additionally, the significance of the RW covariate was evaluated using Wald-type test statistics (Pinheiro and Bates, 2000).

The final step in model development was to investigate the possibility of regional effects on the pith-to-bark patterns for EWD, LWD, LWP and RD. Using Cranbrook as the reference site, we tested for a significant difference between the reference site and each other site. Using the β_1 parameter in equation (4) as an example, this test was incorporated into the above models using the following notation

$$\beta_1 = \beta_{1,\mathrm{CR}} + \beta_{1,\mathrm{Site}}, \tag{8}$$

where $\beta_{1,\mathrm{CR}}$ is the reference value for parameter β_1 and $\beta_{1,\mathrm{Site}}$ is the difference between the reference value and that for any other site. Site- and tree-level random effects were included on all fixed-effect parameters during model development. However, random effects were dropped if their standard deviation was small relative to the associated fixed effect or if pairs of random effects were highly correlated (Pinheiro and Bates, 2000). All equations were fitted using maximum likelihood through the nlme package (Pinheiro *et al.*, 2015) for R (R Core Team, 2013).

Following Parresol (1999), the overall performance of the final models for EWD, LWD, LWP and RD were evaluated using adjusted pseudo-R^2. Mean error bias (bias), absolute percent bias (per cent$|E|$) and root mean square error (RMSE) were also calculated. Finally, we calculated per cent$|E|$ for the following ring-groups: 2–20, 21–40 and 41–60, which was used to assess model performance at different stages along the pith-to-bark gradient.

Component model vs *direct estimation of RD*

The component model calculation of annual RD combines conditional errors from three separate models. Consequently, an examination into the propagation of errors was necessary. We first considered conducting an in-depth error propagation analysis. However, for the purposes of this study, we simply needed assurances that the errors from the combined models were additive rather than multiplicative. Therefore, an examination of error bounds was performed under the assumption that the normal distribution which was observed for each ring component was representative of the population. Results of the analysis are provided as Supplementary data Material and indicate that the combination of error terms resulting from the component model approach are indeed additive and should be on the same order of magnitude as those resulting from a direct estimate of annual RD.

With these assurances, a component model estimate of annual RD was calculated following equation (3). The performance of the component model approach was then compared with the direct estimate of annual RD through pseudo-R^2, RMSE, bias and per cent$|E|$.

Results

The pith-to-bark patterns for annual RD and EWD showed considerable variability between trees at all sites. Conversely, pith-to-bark patterns for LWD and LWP showed greater consistency from tree to tree. At the site level, the pith-to-bark pattern for annual RD showed the least amount of similarity across sites. The pattern at the CR, MC and PA sites was for annual RD to show a sharp decline from the pith followed by a gradual increase with RN from pith. This differed from the pattern at the MK, TN and TF sites which consisted of a moderate decrease in annual RD with RN.

Model for annual EWD

According to AIC and the likelihood ratio test, the best model for annual EWD was obtained after the β_2 parameter in equation (4) was allowed to vary as a function of RW (likelihood ratio test statistic = 853.48, $P < 0.01$). The final model for annual EWD, including random effects, was

$$\mathrm{EWD}_{ijk} = \beta_0 \times \exp[(-\beta_1 + b_{1,j}) \times \mathrm{RN}_{ijk}] + \frac{(\beta_2 + b_{2,j} + \beta_4 \times \mathrm{RW}_{ijk}) \times \mathrm{RN}_{ijk}}{(\beta_3 + \mathrm{RN}_{ijk})} + \varepsilon_{ijk}, \tag{9}$$

where all variables are as previously defined and the estimated parameters are listed in Table 2. The parameter associated with the RW covariate was significant as indicated by the Wald-type test statistic. The model predicts that increased radial growth rate will result in a decrease in EWD within the section of the stem containing mature wood (Figure 1).

The CR and PA sites showed similar pith-to-bark patterns for annual EWD given that tests of the site-specific estimates for the β_1 and β_2 parameters indicated that there were no significant differences between these two sites. Conversely, estimated parameters for β_1 and β_2 for all sites east of the continental divide were significantly lower than that of the CR site.

The final model for annual EWD included tree-level random effects on both the β_1 and β_2 parameters as they provided a significant improvement in model performance. Correlation among the tree-level random effects was weak suggesting that an appropriate covariance structure was used and that over-parameterization was unlikely. Site-level random effects did not improve the model, which was not surprising given the use of site-specific fixed-effect parameters. Fit statistics indicated that the fixed component of the model explained 24 per cent of the variability and tended to slightly underestimate EWD (bias = 2.95). Values for per cent$|E|$ were relatively similar for all three ring-groups. Bias was essentially eliminated when tree-level random effects were considered (bias = 0.017) (Table 4).

Model for annual LWD

For the prediction of annual LWD, the best model was achieved once a covariate for RW was included as an additive effect on the γ_2 parameter (likelihood ratio test statistic = 111.86, $P \leq 0.01$). The test statistic indicated that the parameter associated with

Table 2 Parameter estimates with standard error in parentheses for fixed-effects and standard deviation of random effects and residuals for the three component models of annual ring density (RD)

Component	Earlywood density		Latewood density		Latewood proportion	
	Parameter	Estimate (SE)	Parameter	Estimate (SE)	Parameter	Estimate (SE)
Fixed effects	β_0	412.16 (7.97)	γ_0	−207.24 (6.46)	δ_0	17.27 (0.55)
					$\delta_{0,\mathrm{PA}}$	3.29 (0.74)
					$\delta_{0,\mathrm{MK}}$	8.51* (0.70)
					$\delta_{0,\mathrm{TF}}$	6.77* (0.69)
					$\delta_{0,\mathrm{MC}}$	5.37* (0.59)
					$\delta_{0,\mathrm{TN}}$	7.89* (0.68)
	β_1	0.41 (0.02)	γ_1	0.24 (0.01)	δ_1	9.53 (0.76)
	$\beta_{1,\mathrm{PA}}$	−0.02 (0.02)			$\delta_{1,\mathrm{PA}}$	1.52 (1.19)
	$\beta_{1,\mathrm{MK}}$	−0.12* (0.02)			$\delta_{1,\mathrm{MK}}$	−8.24* (1.11)
	$\beta_{1,\mathrm{TF}}$	−0.09* (0.02)			$\delta_{1,\mathrm{TF}}$	−8.04* (1.13)
	$\beta_{1,\mathrm{MC}}$	−0.07* (0.02)			$\delta_{1,\mathrm{MC}}$	−4.08* (0.96)
	$\beta_{1,\mathrm{TN}}$	−0.19* (0.02)			$\delta_{1,\mathrm{TN}}$	−9.64* (1.11)
	β_2	470.89 (4.57)	γ_2	−0.81 (0.07)	δ_2	29.79 (0.48)
	$\beta_{2,\mathrm{PA}}$	1.73 (7.64)				
	$\beta_{2,\mathrm{MK}}$	−18.08* (6.96)				
	$\beta_{2,\mathrm{TF}}$	−17.52* (6.88)				
	$\beta_{2,\mathrm{MC}}$	−40.67* (5.90)				
	$\beta_{2,\mathrm{TN}}$	−33.75* (6.88)				
	β_3	0.83 (0.06)	γ_3	847.14 (7.21)	δ_3	4.05 (0.41)
			$\gamma_{3,\mathrm{PA}}$	7.02 (11.02)		
			$\gamma_{3,\mathrm{MK}}$	−24.22* (10.01)		
			$\gamma_{3,\mathrm{TF}}$	−78.39* (9.93)		
			$\gamma_{3,\mathrm{MC}}$	−126.40* (8.54)		
			$\gamma_{3,\mathrm{TN}}$	−77.89* (9.85)		
	β_4	−18.36 (0.62)	γ_4	0.52 (0.05)	γ_4	−0.55 (0.12)
Random effects	$\sigma_{\mathrm{b}1,j}$	0.10	$\sigma_{\gamma 3,j}$	46.41	$\sigma_{\delta 0,j}$	2.68
	$\sigma_{\mathrm{b}2,j}$	32.91			$\sigma_{\delta 1,j}$	4.47
	$\sigma_{\mathrm{Residual}}$	33.32	$\sigma_{\mathrm{Residual}}$	78.45	$\sigma_{\mathrm{Residual}}$	6.82

Subscripts *i*, *j* and *k* denote the site, tree and ring, respectively.
All parameters are significant ($P < 0.01$); asterisk (*) is used on site-specific parameters only and denotes a significant difference from the base parameter for the CR site. The CR and PA sites are on the western slopes of the Rockies, whereas MK, TF, MC and TN are on the eastern slopes.

RW was significant. A tree-level random effect for γ_3 (i.e. $c_{3,j}$) was retained in the final model as it significantly improved model performance. The final equation for annual LWD was

$$\mathrm{LWD}_{ijk} = \gamma_0 \times \exp(-\gamma_1 \times \mathrm{RN}_{ijk}) + (\gamma_2 + \mathrm{RW}_{ijk} \times \gamma_4) \times \mathrm{RN}_{ijk} + \gamma_3 + c_{3,j} + \varepsilon_{ijk} \quad (10)$$

where all variables are as previously defined and estimated parameters are presented in Table 2. Based on parameter estimates, annual LWD is expected to increase with increasing radial growth rate (Figure 2).

As with EWD, there were similarities in the pith-to-bark patterns for LWD at the CR and PA sites given that no significant differences were found in the site-specific estimates for the γ_3 parameter for these two sites. However, the same tests indicated that the γ_3 parameter for all sites on the eastern slopes of the Rocky Mountains were significantly lower than the CR site. The variability explained by the fixed-effect component of the model was 29 per cent, increasing to 49 per cent with use of both fixed and random effects. There was little overall bias in predictions resulting from the fixed-effect component of the LWD model (bias = 0.12) (Table 4). Following the addition of tree-level random effects, values for per cent$|E|$ within ring group 20–40 showed the greatest improvement relative to the other ring groups.

Model for annual LWP

For annual LWP, allowing the δ_0 parameter to vary as a function of RW provided a significant improvement in model performance over the next best model (likelihood ratio test statistic = 16.39, $P <$ 0.01). The parameter for RW was significant according to the Wald-type test and indicated that increased growth rate should result in an overall decrease in LWP from pith to bark (Figure 3). The final model was

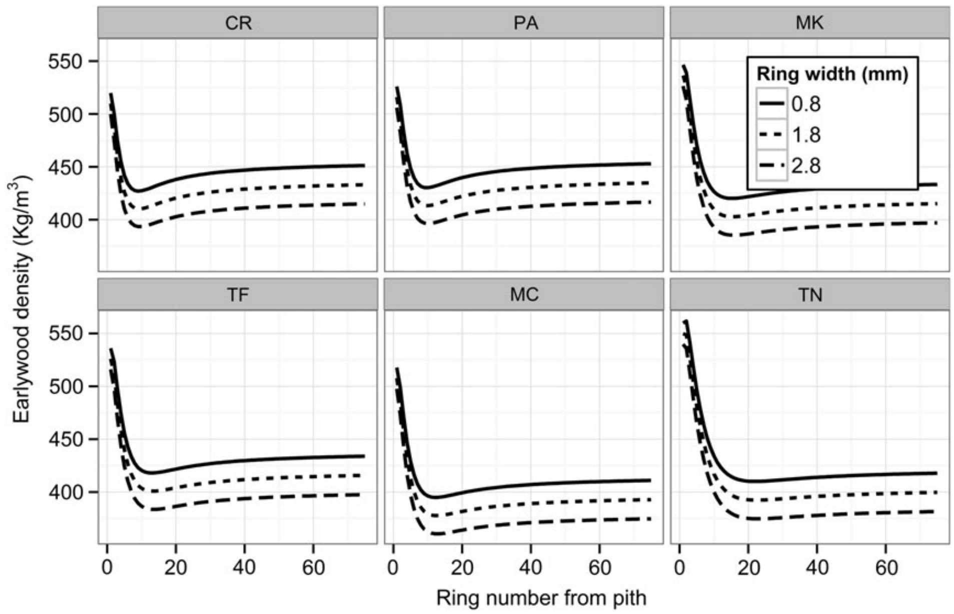

Figure 1 Model predictions for earlywood density for three levels of ring width (mm year^{-1}). Cranbrook (CR) and Parsons (PA) are on the western slopes of the Rockies. MacKay (MK), Teepee flats (TF), McCardell (MC) and Teepee north (TN) are on the eastern slopes.

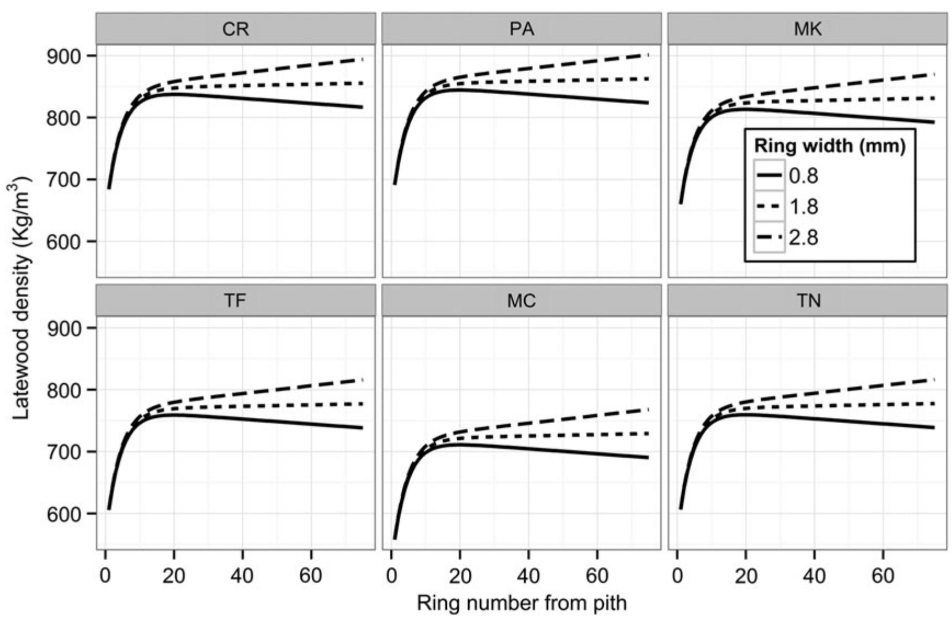

Figure 2 Model predictions for latewood density for three levels of ring width (mm year^{-1}). CR and PA are on the western slopes of the Rockies. MK, TF, MC and TN are on the eastern slopes.

$$\mathrm{LWP}_{ijk} = (\delta_0 + d_{0,j} + \delta_4 \times \mathrm{RW}_{ijk}) + \frac{\delta_1 + d_{1,j}}{1 + \exp\left[\dfrac{(\delta_2 - \mathrm{RN}_{ijk})}{\delta_3}\right]} + \varepsilon_{ijk}. \quad (11)$$

All variables in equation (11) remain as previously defined with estimated parameters presented in Table 2. As with the models for EWD and LWD, including tree-level random effects provided significant improvement over a reduced model with only fixed effects. Specifically, random effects on the δ_0 and δ_1 parameters (i.e. $d_{0,j}$ and $d_{1,j}$) provided the greatest overall model improvement. No improvement was obtained by including site-level random effects.

Contrasts of the site-specific δ_0 parameter indicated that all sites were significantly different from the CR site. However, the pith-to-bark pattern in LWP at the PA site showed greater

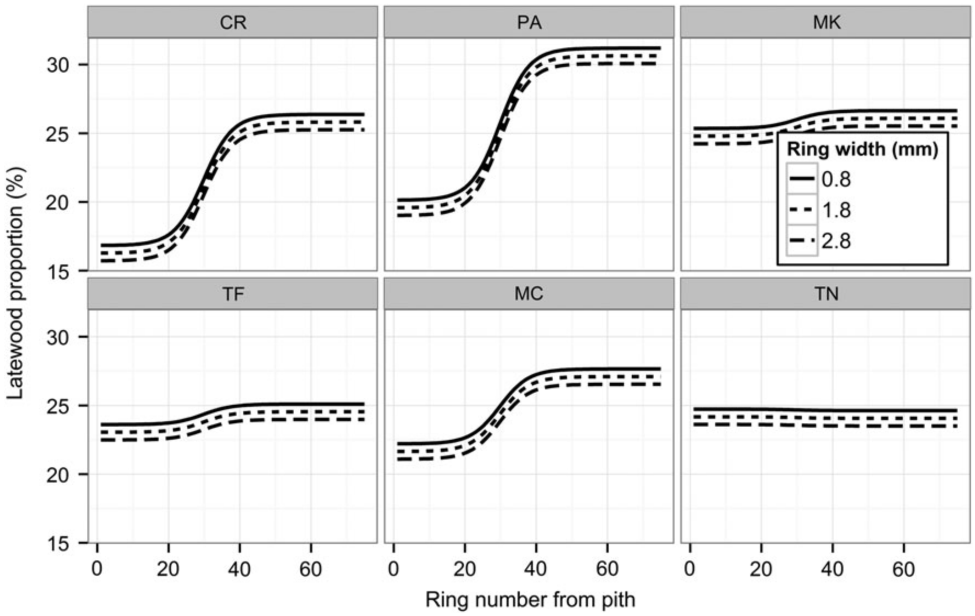

Figure 3 Model predictions for latewood proportion for three ring widths (mm year^{-1}). CR and PA are on the western slopes of the Rockies. MK, TF, MC and TN are on the eastern slopes.

similarity to the CR site given that the δ_1 parameter was not significantly different from the reference site. For all sites on the eastern slopes of the Rockies, LWP was significantly lower than the reference site.

The total variability explained by the model for annual LWP with both fixed and random effects was the lowest among the three components of RD that we modelled (Table 4). Overall, the model was relatively unbiased (bias = −0.05). Based on values for per cent|E| by ring-group, most of the between-tree variability appeared to lie between rings 40–60 given that this ring group showed the greatest improvement in per cent|E| following the addition of tree-level random effects.

Direct estimation of annual RD

Efforts to improve the starting-point model for the direct estimate of annual RD proved unsuccessful. Parameters failed to converge following multiple attempts at including a covariate for RW. Likewise, parameters failed to converge when site-specific fixed effects were requested. Thus, the final model for the direct estimate of annual RD was

$$\mathrm{RD}_{ijk} = \phi_0 \times \exp[-(\phi_1 + g_{1,i} + g_{1,ij}) \times \mathrm{RN}_{ijk}] + \frac{(\phi_2 + g_{2,i} + g_{2,ij}) \times \mathrm{RN}_{ijk}}{(\phi_3 + \mathrm{RN}_{ijk})} + \varepsilon_{ijk}, \qquad (12)$$

where all variables are as previously defined and estimated parameter are listed in Table 3. Random effects at the site- and tree-level for the ϕ_1 and ϕ_2 parameters were retained as they significantly improved model performance. The variability in annual RD explained by the fixed-effect component of the model was only 5 per cent, with an additional 50 per cent of the variability being explained through the addition of the site and tree-level random effects (Table 4).

Table 3 Parameter estimates for the direct estimate of annual RD (equation (12)) with standard error in parentheses and standard deviation of random effects and residuals

Component	Parameter	Estimate (SE)
Fixed effects	ϕ_0	443.82 (9.08)
	ϕ_1	0.19 (0.03)
	ϕ_2	560.85 (12.89)
	ϕ_3	3.61 (0.21)
Random effects	$\sigma_{g1,i}$	0.06
	$\sigma_{g1,ij}$	<0.01
	$\sigma_{g2,i}$	30.07
	$\sigma_{g2,ij}$	44.91
	$\sigma_{\mathrm{Residual}}$	46.96

Subscripts i, j and k denote the site, tree and ring, respectively.

Component vs *direct estimate of annual RD*

Using only the fixed-effect components of the models for EWD, LWD and LWP, estimates of annual RD generated through equation (3) showed a tendency to overestimate annual RD at low levels of observed RD and to underestimate RD at high levels of observed RD (Figure 4). This tendency was more pronounced for estimates of annual RD from equation (12). When tree-level random effects were included, predictions from the component model approach and the direct approach showed similar agreement with observed values of annual RD.

All fit statistics indicated that the component model approach to estimate annual RD was superior to that of the direct approach (Table 4). The sole exception was that bias was slightly smaller for the direct estimate of RD when using both fixed and random effects.

Table 4 Fit statistics and measures of bias for the three ring component models (equations (9)–(11)), annual ring density from equation (3) and the direct estimate of annual ring density (equation (12))

Equation	Adjusted R^2	RMSE	Bias	%|E|	%|E| 2–20	20–40	40–60
Earlywood density (equation (9))	24 (63)	46.25 (31.94)	2.95 (0.02)	8.34 (5.62)	8.45 (5.65)	8.12 (5.36)	8.51 (5.6)
Latewood density (equation (10))	29 (49)	91.18 (76.94)	0.12 (−0.05)	9.34 (7.85)	9.56 (8.59)	8.67 (6.86)	9.84 (8.61)
Latewood proportion (equation (11))	16 (37)	7.75 (6.63)	−0.04 (−0.04)	24.41 (20.66)	26.27 (23.49)	22.57 (19.13)	24.31 (19.08)
RD (equation (3))	25 (64)	59.45 (41.81)	1.14 (−0.86)	9.13 (6.36)	8.57 (6.23)	9.10 (6.19)	9.68 (6.49)
RD (equation (12))	5 (55)	67.02 (45.26)	3.85 (0.31)	10.43 (6.89)	10.50 (7.53)	10.11 (6.37)	10.68 (6.67)

RMSE = root mean square error, $\%|E|$ = absolute mean percent bias.
RMSE (kg m^{-3}), $\%|E|$, and bias are from predictions using the fixed-effect component of the equations. Fit statistics from both fixed and random effects are given in parentheses.

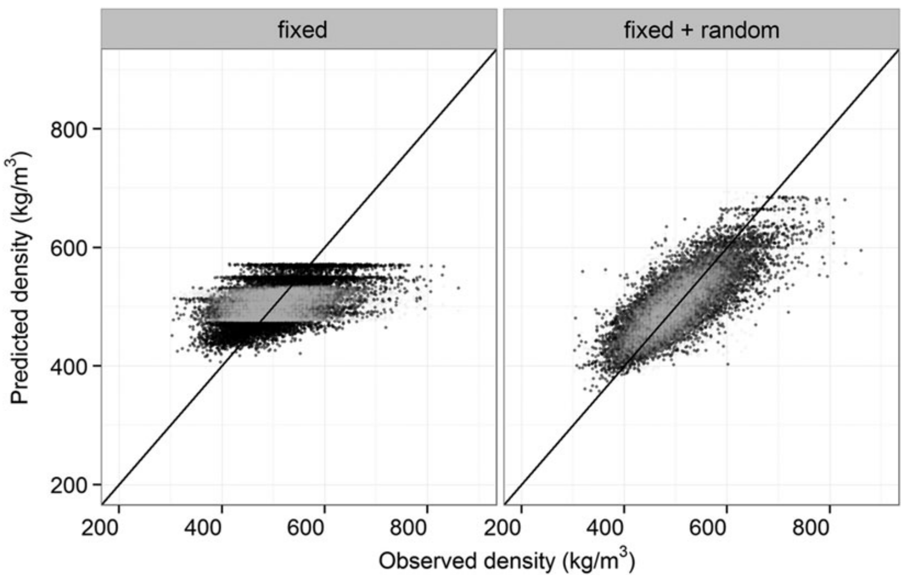

Figure 4 Observed *vs* predicted values of annual ring density derived a component model approach (black dots) and a direct approach (grey dots). CR and PA are on the western slopes of the Rockies. MK, TF, MC and TN are on the eastern slopes.

Discussion

EWD model

Although a simpler equation form to describe annual EWD was sought, none of the alternative equations we tested provided sufficient flexibility. The placement of the RW covariate in the final model indicates that the effect of RW on annual EWD is weak in the juvenile wood core but becomes stronger as the tree ages. This result is in accordance with the reports from both red pine (Larocque and Marshall, 1995) and jack pine (Schneider *et al.*, 2008), where radial growth rate was found to have little effect on EWD within the juvenile wood core at BH. Larocque and Marshall (1995) go on to point out that trends in EWD for red pine began to diverge beyond a cambial age at BH of about 25 years. For lodgepole pine, it appears that significant divergence in pith-to-bark trends for EWD occur up to 10 years earlier (Figure 1).

When radial growth rate is high, there is a greater presence of growth-regulating hormones during earlywood formation which results in the production of large, thin-walled cells (Larson, 1969). This change in cell structure has been used to link increased radial growth rate with a decrease in EWD. Although non-significant or weak negative relationships between RW and annual EWD have been reported for some species of pine (Antony et *al.*, 2011), this may partially be due to a narrow range of RW in the sample dataset. The significant negative effect of RW on annual EWD that was found for lodgepole pine is consistent with most findings from other North American species of pine (Larocque and Marshall, 1995; Schneider *et al.*, 2008; Savva et *al.*, 2010). For Scots pine, Peltola *et al.* (2007) noted that heavily thinned stands had lower overall EWD, presumably a result of increased growth rate following thinning.

LWD model

The placement of the RW covariate in the model implies that annual RW has its greatest effect on LWD in the mature wood where mean annual RW was ~1.5 mm year^{-1}. The overall positive relationship between RW and LWD reported here is similar to findings reported for jack pine (Schneider *et al.*, 2008) where it was noted that the relationship was strongest when annual RW was <2 mm year^{-1}. Savva *et al.* (2010) for jack pine and Zhu *et al.* (2007) for red pine also noted a positive relationship between RW and LWD.

Despite the supporting evidence, there is no strong consensus that RW is positively correlated with LWD within pine species. Larocque and Marshall (1995), for example, reported little-to-no effect of RW on LWD for red pine. More recently, Mäkinen and Hynynen (2014) reported that thinning treatments, which affected RW, had no effect on LWD for Scots pine. The absence of an effect of RW on LWD has also been reported for several other conifers, including western hemlock (*Tsuga heterophylla* (Raf.) Sarg.) (DeBell *et al.*, 1994), balsam fir (*Abies balsamea* (L.)) (Koga and Zhang, 2004) and Norway spruce (*Picea abies* (L.) Karst.) (Jaakkola *et al.*, 2005).

For the current study, the method by which the earlywood–latewood boundary was defined may, in part, have influenced the strength of the relationship between RW and LWD. This is because the maximum intra-annual density varies more than the minimum intra-annual density (Bouriaud *et al.*, 2005; Jyske *et al.*, 2008). Since maximum intra-annual density is reported to be positively correlated with RW, an increase in RW will increase maximum intra-annual density more than it will decrease minimum density (Melvin *et al.*, 2013; Pritzkow *et al.*, 2014). According to the definition of the earlywood-to-latewood transition point used here, this would imply a shift in the earlywood–latewood boundary away from the pith within a given ring. This would result in a higher average density for the latewood proportion. Such an effect would, therefore, magnify the positive relationship between annual RW and LWD. To determine the extent to which the current measurement of the earlywood–latewood boundary affects the LWD-RW relationship, one could evaluate the model under different definitions of the earlywood–latewood boundary. These factors should be taken into consideration in future studies.

LWP model

The placement of the RW covariate in the model implies that radial growth rate affects LWP at all stages of tree growth. The decrease in LWP with increasing annual RW is consistent with studies from jack pine (Schneider *et al.*, 2008) and Scots pine (Mäkinen and Hynynen, 2012). However, as is the case with LWD, there is no consensus that RW has an effect on LWP. For example, in contrast to earlier work on Scots pine, Mäkinen and Hynynen (2014) reported that thinning treatments which increased radial growth rates had little effect on LWP. Likewise, Tasissa and Burkhart (1998) reported that LWP within loblolly pine (*P. taeda* L.) was unrelated to thinning intensity which was positively correlated with the radial growth rate.

Among the three components we modelled, LWP is reported to be the most important determinant of annual RD (Megraw, 1985; Tasissa and Burkhart, 1998; Mäkinen *et al.*, 2007; Schneider *et al.*, 2008). Thus, it was discouraging that the fixed-effect component of the model explained such a low proportion of the total variability in LWP. The performance of the model was, however, comparable to that reported by Mäkinen *et al.* (2007) for LWP in Norway spruce.

Regional differences

Results for the current study consistently indicated that the pith-to-bark trends for annual EWD, LWD and LWP for sites on the western slopes of the Canadian Rock Mountains behaved differently than those on the eastern slopes. In general, values for annual EWD, LWD and LWP tended to be higher in the sites on the western slopes. Owing to the rain shadow effect, the eastern slopes of the Rocky Mountains are drier than the western slopes which may affect the development of cell tracheids. However, for both red pine and jack pine, drier conditions have been correlated with an increase in EWD and LWD (Larocque, 1997; Savva *et al.*, 2010). Conversely, the warmer mean annual temperatures on the western slopes may lead to increases in EWD and LWD, a trend which had previously been reported for Scots pine (Tuovinen, 2004; Kilpeläinen et al., 2005). For a clearer indication of how climate influences the components of annual RD in lodgepole pine, climate variables will need to be tested in future versions of the models. Regional climatic differences aside, the clear distinction between the sites on the western slopes from those on the eastern slopes is important as it will serve as a starting point from which to define regional calibration zones for the component models.

Component vs *direct estimate of annual RD*

The equations for EWD, LWD and LWP appear complex. This contrasts with our initial expectations that using a component model approach would simplify both the equation forms and the model-fitting process. However, they are more parsimonious than the RD component models presented by Schneider *et al.* (2008) for jack pine and reflect the variable relationship that each component of annual RD has with cambial age and RW. Together, the models indicate that, for lodgepole pine, radial growth rate influences the development of tracheid cells throughout the growing season. The negative relationship between RW and annual EWD suggest that in the early half of the growing season, an increase in growth rate causes lumen diameters to increase. In contrast, the positive relationship between RW and LWD suggests that there is a thickening of cell walls in response to an increase in growth rate during the latter half of the season.

The fit statistics presented in Table 4 clearly support the use of a component modelling approach. However, the comparison of the two modelling approaches was somewhat limited by the inability to test covariates for RW and site effects in the model for the direct estimation of RD. The issues related to parameter convergence are likely the result of the high inter-annual variability and the high between-tree variability in annual RD. Even after relaxing various parameters used by the estimation algorithm, we could not resolve convergence problems. In contrast, fitting the models for EWD, LWD and LWP was relatively straightforward, which seems to support our assertion that a component modelling approach will facilitate the model-fitting process.

Similar to the annual RD model provided by Peng and Stewart (2013), the models for EWD, LWD and LWP are expected to provide reasonably good estimates of RD if the random effects for a 'new' stand can be estimated. Random effects can be estimated for a 'new' stand if a sample of trees within the stand is measured for annual EWD, LWD and LWP. However, in forestry, a scenario such as this is rare. Most often, the prediction of annual EWD, LWD, LWP or RD will be required for stands which have no prior measurement, meaning that predictions can be derived using only the estimated parameters for the fixed effects. In this respect, the component models presented here are expected to calculate annual RD with slightly greater accuracy than the model presented by Peng and Stewart (2013).

Conclusion

In the current study, we developed models for annual EWD, LWD and LWP for lodgepole pine. When combined, estimates from these three models can be used to derive annual RD from pith to bark. There was a significant effect of RW in all three models, with EWD and LWP decreasing and LWD increasing with increased growth rate. Furthermore, similarities between sites on the western slopes of the Rockies for all three ring components point toward the presence of regional climatic effects, although there remains a need to explicitly examine the influence of latitude, altitude, temperature and precipitation. We found the derivation of annual RD from models for EWD, LWD and LWP to be superior to a direct estimation of annual RD in terms of both model-fitting and overall-fit statistics. The models are designed to use as their input the annual output provided by tree growth simulators. Thus, their application within a forest management context will be through their inclusion into a software package which currently includes models to predict the transition from juvenile wood to mature wood (Wang and Stewart, 2012;2013). This software is designed to link with individual tree growth simulators such as the Mixedwood Growth Model (Bokalo *et al.*, 2013).

Supplementary data

Supplementary data are available at *Forestry* online.

Acknowledgements

The authors thank Jared Salvail, John Vallentgoed, Jonathan Martin DeMoor, Dominique Lejour, Calvin Strom, Kirsten Mortensen and Myriam Suard (Canadian Wood Fibre Centre) for carrying out the field work for this project. The support of Sharon Meredith (Foothills Growth and Yield Association) was instrumental in carrying out this research. Comments on earlier versions of the manuscript by Isabelle Duchesne, Cosmin Filipescu, Art Groot and three anonymous reviewers are greatly appreciated.

Conflict of interest statement

None declared.

Funding

This work was supported by the Canadian Wood Fibre Centre, Canadian Forest Service, Natural Resources Canada; and the Foothills Growth and Yield Association.

References

Akaike, H. 1974 New look at statistical-model identification. *IEEE Trans. Autom. Control* **19**, 716–723. AC.

Antony, F., Schimleck, L.R., Daniels, R.F. and Clark, A. III. 2011 Effect of fertilization on growth and wood properties of thinned and unthinned midrotation Loblolly pine (*Pinus taeda* L.) stands. *South. J. Appl. For.* **35**, 142–147.

Auty, D., Achim, A., Macdonald, E., Cameron, A.D. and Gardiner, B.A. 2014 Models for predicting wood density variation in Scots pine. *Forestry* **87**, 449–458.

Barbour, R.J., Fayle, D.C.F., Chauret, G., Cook, J., Karsh, M.B. and Ran, S. 1994 Breast-height relative density and radial growth in mature jack pine (*Pinus banksiana*) for 38 years after thinning. *Can. J. For. Res.* **24**, 2439–2447.

Bokalo, M., Stadt, K., Comeau, P. and Titus, S. 2013 The validation of the Mixedwood Growth Model (MGM) for use in forest management decision making. *Forests* **4**, 1–27.

Bouriaud, O., Leban, J.-M., Bert, D. and Deleuze, C. 2005 Intra-annual variations in climate influence growth and wood density of Norway spruce. *For. Ecol Manage.* **25**, 651–660.

DeBell, J.D., Tappeiner, J.C. II and Krahmer, R.L. 1994 Wood density of western hemlock: effect of ring width. *Can. J. For. Res.* **24**, 638–641.

Defo, M., Goodison, A. and Uy, N. 2009 A method to map within-tree distribution of fibre properties using SilviScan-3 data. *For. Chron.* **85** (3), 409–414.

Evans, R. 1994 Rapid measurement of the transverse dimensions of tracheids in radial wood sections from Pinus radiata. *Holzforschung* **48** (2), 168–172.

Jaakkola, T., Mäkinen, H. and Saranpää, P. 2005 Wood density in Norway spruce: changes with thinning intensity and tree age. *Can. J. For. Res.* **35**, 1767–1778.

Jyske, T., Mäkinen, H. and Saranpää, P. 2008 Wood density within Norway spruce stems. *Silva Fennica* **42** (3), 439–455.

Kilpeläinen, A., Peltola, H., Ryyppö, A. and Kellomäki, S. 2005 Scots pine responses to elevated temperature and carbon dioxide concentration: growth and wood properties. *Tree Physiol.* **25**, 75–83.

Koga, S. and Zhang, S.Y. 2004 Inter-tree and intra-tree variations in ring width and wood density components in balsam fir (*Abies balsamea*). *Wood Sci. Technol.* **38**, 149–162.

Larocque, G.R. 1997 Importance de différents paramètres climatique sur la croissance et la formation du bois de pin rouge (*Pinus resinosa* Ait) en Ontario (Canada). *Ann. Sci. For.* **54**, 51–63.

Larocque, G.R. and Marshall, P.L. 1995 Wood relative density development in red pine (*Pinus resinosa* Ait.) stands as affected by different initial spacings. *For. Sci.* **41**, 709–728.

Larson, P.R. 1969 Wood formation and the concept of wood quality. *Bull. Yale School For.* **74**, 54.

Mäkinen, H. and Hynynen, J. 2012 Predicting wood and tracheid properties of Scots pine. *For. Ecol. Manage.* **279**, 11–20.

Mäkinen, H. and Hynynen, J. 2014 Wood density and tracheid properties of Scots pine: responses to repeated fertilization and timing of the first commercial thinning. *Forestry* **87**, 437–447.

Mäkinen, H., Jaakkola, T., Piispanen, R. and Saranpää, P. 2007 Predicting wood and tracheid properties of Norway spruce. *For. Ecol. Manage.* **241**, 175–188.

Mansfield, S.D., Parish, R., Goudie, J.W., Kang, K.-Y. and Ott, P. 2007 The effects of crown ratio on the transition from juvenile to mature wood production in lodgepole pine in western Canada. *Can. J. For. Res.* **37**, 1450–1459.

Mansfield, S.D., Parish, R., Di Lucca, C.M., Goudie, J., Kang, K.-Y. and Ott, P. 2009 Revisiting the transition between juvenile and mature wood: a comparison of fibre length, microfibril angle and relative wood density in lodgepole pine. *Holzforschung* **63**, 449–456.

Megraw, R.A. 1985 *Wood Quality Factors in Loblolly Pine. The Influence of Tree Age, Position in Tree, and Cultural Practice on Wood Specific Gravity, Fiber Length, and Fibril Angle*. TAPPI Press, 88 pp.

Middleton, G.R., Munro, B.D., Jozsa, L.A., Palka, L.C. and Sen, P. 1995 Lodgepole pine product yields related to differences in stand density. Special publication – Forintek Canada Corporation (Canada). 0824–2119, no. SP-35, 65 pp.

Melvin, T.M., Grudd, H. and Briffa, K.R. 2013 Potential bias in 'updating' tree-ring chronologies using regional curve standardization: Re-processing 1500 years of Torneträsk density and ring-width data. *Holocene* **23** (3), 364–373.

Parresol, B.R. 1999 Assessing tree and stand biomass: a review with examples and critical comparisons. *For. Sci*. **45**, 573–593.

Peltola, H., Kilpeläinen, A., Sauvala, K., Räisänen, T. and Ikonen, V.-P. 2007 Effects of early thinning regime and tree status on the radial growth and wood density of Scots pine. *Silva Fenn*. **41** (3), 489–505.

Peng, M. and Stewart, J.D. 2013 Development, validation, and application of a model of intra- and inter-tree variability of wood density for lodgepole pine in western Canada. *Can. J. For Res*. **43**, 1172–1180.

Pinheiro, J.C. and Bates, D.M. 2000 *Mixed-effects Models in S and S-PLUS*. Springer, 528pp.

Pinheiro, J., Bates, D., DebRoy, S. and Sarkar, D., and R Core Team. 2015 nlme: Linear and Nonlinear Mixed Effects Models. R package version 3.1–120.

Pritzkow, C., Heinrich, I., Grudd, H. and Helle, G. 2014 Relationship between wood anatomy, tree-ring widths and wood density of *Pinus sylvestris* L. and climate at high latitudes in northern Sweden. *Dendrochronologia*. **32**, 295–302.

R Core Team. 2013 R: A Language and Environment for Statistical Computing. R Foundation for Statistical Computing, Vienna, Austria. URL: http://.R-project.org.

Savva, Y., Koubaa, A., Tremblay, F. and Bergeron, Y. 2010 Effects of radial growth, tree age, climate, and seed origin on wood density of diverse jack pine populations. *Trees*. **24** (1), 53–65.

Schneider, R., Zhang, S., Swift, D.E., Bégin, J. and Lussier, J.-M. 2008 Predicting selected wood properties of jack pine following commercial thinning. *Can. J. For. Res*. **38**, 2030–2043.

Stewart, J.D., Jones, T.N. and Noble, R.C. 2006 *Long-term Lodgepole Pine Silviculture Trials in Alberta: History and Current Results*. Natural Resources Canada, Canadian Forest Service and Foothills Model Forest, 184 pp.

Tasissa, G. and Burkhart, H. 1998 Modelling thinning effects on ring specific gravity of loblolly pine (*Pinus taeda* L.). *For. Sci*. **44** (2), 212–223.

Tuovinen, M. 2004 Response of tree-ring width and density of *Pinus sylvestris* to climate beyond the continuous norther forest line in Finland. *Dendrochronologia*. **22**, 83–91.

Wang, T. and Aitken, S.N. 2001 Variation in xylem anatomy of selected populations of lodgepole pine. *Can. J. For. Res*. **31**, 2049–2057.

Wang, M. and Stewart, J. 2012 Determining the transition from juvenile to mature wood microfibril angle in lodgepole pine: a comparison of six different two-segment models. *Ann. For. Sci*. **69**, 927–937.

Wang, M. and Stewart, J.D. 2013 Modeling the transition from juvenile to mature wood using modulus of elasticity in lodgepole pine. *West. J. Appl. For*. **28**, 135–142.

Wang, T., Aitken, S.N., Rozenberg, P. and Millie, F. 2000 Selection of improved growth and wood density in lodgepole pine: effects on radial patterns of wood variation. *Wood Fiber Sci*. **32**, 391–403.

Whitehead, R.J. and Russo, G.L. 2005 Beetle-proofed lodgepole pine stands in interior British Columbia have less damage from mountain pine beetle. Information Report BC-X-402. Natural Resources Canada, Canadian Forest Service, Pacific Forestry Centre, 17 pp.

Wilhelmsson, L., Arlinger, J., Spangberg, K., Lundqvist, S.O., Grahn, T., Hedenberg, O. and Olsson, L. 2002 Models for predicting wood properties in stems of *Picea abies* and *Pinus sylvestris* in Sweden. *Scand. J. For. Res*. **17**, 330–350.

Zhu, J., Scott, C., Scallon, K. and Myers, G. 2007 Effects of plantation density on wood density and anatomical properties of red pine (*Pinus resinosa* Ait.). *Wood Fiber Sci*. **39**, 502–512.